Photosensitizer verteporfin inhibits the growth of YAP- and TAZ-dominant gastric cancer cells by suppressing the anti-apoptotic protein Survivin in a light-independent manner

TAKASHI HASEGAWA*, TAKAAKI SUGIHARA*, YOSHIKI HOSHINO, RYOHEI TARUMOTO, YUKAKO MATSUKI, TSUTOMU KANDA, TOMOAKI TAKATA, TAKAKAZU NAGAHARA, TOMOMITSU MATONO and HAJIME ISOMOTO

Division of Medicine and Clinical Science, Department of Gastroenterology and Nephrology, School of Medicine, Faculty of Medicine, Tottori University, Yonago 683-8504, Japan

Received January 20, 2021; Accepted July 7, 2021

DOI: 10.3892/ol.2021.12964

Abstract. Yes-associated protein (YAP) positivity indicates a poor prognosis in gastric cancer. Transcriptional co-activator with a PDZ-binding domain (TAZ), a YAP paralog, is highly expressed in gastric signet ring cell carcinoma. Verteporfin (VP), a clinical photosensitizer, was recently shown to inhibit YAP/TAZ. In the present study, the therapeutic potential of VP treatment was explored using two gastric cancer cell lines: MKN-45 (TAZ-dominant) and MKN-74 (YAP-dominant). Cell proliferation was evaluated by MTS assay. Vascular mimicry was evaluated by the tube formation assay. Gene and protein expression levels of YAP/TAZ downstream effectors [such as Survivin, Cysteine-rich angiogenic inducer 61 (CYR61), and connective tissue growth factor (CTGF)] were measured. YAP or TAZ localization was evaluated by immunofluorescence. Cell death was assessed by immunofluorescent staining of Annexin V. YAP and TAZ expression were knocked down by small interfering RNA. The current results demonstrate that MKN-45, a poorly differentiated TAZ-dominant gastric cancer cell line, was more sensitive to VP than MKN-74, a moderately differentiated YAP-dominant gastric cancer cell line. VP changed the localization of YAP/TAZ, promoted its degradation and significantly decreased the protein level of Survivin in both cell lines. Cell death was induced by VP treatment in a dose-dependent manner. Vascular mimicry was inhibited in both cell lines. Proliferation in both cell lines decreased in response to YAP/TAZ knockdown. The present study indicated that VP has potential as a therapeutic agent in YAP- and TAZ-dominant gastric cancers due to its ability to suppress the anti-apoptotic protein Survivin via inhibition of YAP and TAZ.

Correspondence to: Dr Takaaki Sugihara, Division of Medicine and Clinical Science, Department of Gastroenterology and Nephrology, School of Medicine, Faculty of Medicine, Tottori University, 36-1 Nishi-cho, Yonago 683-8504, Japan
E-mail: sugitaka@tottori-u.ac.jp

*Contributed equally

Key words: gastric cancer, verteporfin, yes-associated protein, transcriptional co-activator with a PDZ-binding domain, Survivin

Introduction

Gastric cancer has the fifth highest incidence among all cancers according to GLOBOCAN 2020 data. Globally, it is the fourth most frequent cause of death among malignancies (1). Although the incidence of gastric cancer is decreasing, it remains a significant public health problem (2). Gastric cancer is commonly diagnosed at an advanced stage, except in Japan and Korea where routine screening is performed (3,4). The efficacy of chemotherapy for advanced-stage gastric cancer has increased the survival rate in recent years; however, the degree of improvement is unsatisfactory (5,6).

The Hippo signaling pathway is essential in the control of organ size. It consists of a series of serine/threonine kinases and scaffolding proteins that regulate the subcellular localization and activity of the effector proteins yes-associated protein (YAP) and transcriptional co-activator with a PDZ-binding domain (TAZ) (7). Overexpression of YAP is observed frequently in a variety of cancer types (8). YAP expression is elevated in gastric adenocarcinomas, and its knockdown inhibits gastric cancer cell proliferation (9). High levels of YAP in the nucleus have been linked to chemoresistance in various cancer types (10-13). In gastric cancer cells, YAP is associated with cisplatin and trastuzumab resistance (14,15). Upregulation of YAP correlates with progression, metastasis and poor prognosis in patients with gastric carcinoma (16). Moreover, the expression of TAZ, a YAP paralog, is elevated in gastric signet ring cell carcinoma (17).

Targeting YAP and TAZ, individually or in combination, is likely to have a clinical impact on gastric cancer. Verteporfin (VP), a benzoporphyrin derivative, is used in photodynamic therapy (PDT) for exudative age-related macular degeneration; specifically, against choroidal neovascularization (18).

We have recently reported the efficacy of VP in PDT using gastric cancer cells (19). Other previous studies propose that VP may inhibit cancer cell growth in the absence of photoactivation by inhibiting the YAP/TAZ transcriptional enhanced associate domain (YAP/TAZ-TEAD) complex (20-22). In the present study, the aim was to investigate the effects of VP on two gastric cancer cell lines: MKN-45 (TAZ-dominant) and MKN-74 (YAP-dominant).

Materials and methods

Clinical samples and datasets. The gene expression patterns of YAP and TAZ in cancer and normal tissue were compared on the Gene Expression Profiling Interactive Analysis (GEPIA) server developed by the Zhang Lab at Peking University (http://gepia.cancer-pku.cn/). The survival analysis of YAP and TAZ was performed on the Kaplan-Meier Plotter online tool headquartered at the Semmelweis University in Budapest (http://kmplot.com/analysis/index.php?p=service&cancer=gastric). Tissue images are obtained from the Human Protein Atlas (https://www.proteinatlas.org/).

Reagents and antibodies. VP (cat. no. SML0534) was purchased from Sigma-Aldrich; Merck KGaA. The following primary antisera were used for the immunoblotting analysis: Anti-β-actin antibody (cat. no. 13E5; Cell Signaling Technology, Inc.), anti-YAP/TAZ antibody (cat. no. D24E4; Cell Signaling Technology, Inc), anti-Survivin antibody (cat. no. EP2880Y; Abcam), anti-CTGF antibody (cat. no. L-20; Santa Cruz Biotechnology, Inc.), and anti-CYR61/CCN1 antibody (cat. no. ab24448; Abcam). The following primary monoclonal antibodies were used for immunofluorescence: Anti-YAP antibody (cat. no. sc-101199; Santa Cruz Biotechnology, Inc.), anti-TAZ antibody (cat. no. ab84927; Abcam), and anti-CD31 antibody (cat. no. ab28364; Abcam). Horseradish peroxidase (HRP)-conjugated goat anti-mouse IgG (cat. no. ab6789; Abcam) and goat anti-rabbit IgG H&L (cat. no. ab97051; Abcam) were purchased for western blotting. Goat anti-mouse IgG H&L (Alexa Fluor® 488; cat. no. ab150113; Abcam) was purchased for immunofluorescence.

Cell lines and cultures. Kato III (derived from a signet ring cell carcinoma with no further information), NUGC-4 (derived from an adenocarcinoma, poorly differentiated, signet ring cell carcinoma with lymph node metastasis in a 32-year-old female), MKN-45-Luc (derived from a poorly differentiated adenocarcinoma in a 62-year-old female), MKN-74/CMV-Luc cells (derived from a moderately differentiated tubular adenocarcinoma with liver metastasis in a 37-year-old male), and PANC-1 (TAZ-dominant pancreatic cancer cell line) were obtained from the JCRB Cell Bank. The Kato III cell line was grown without antibiotics in Roswell Park Memorial Institute (RPMI)-1640 (FUJIFILM Wako Pure Chemical Corporation) medium with Eagle's minimal essential medium (E-MEM; FUJIFILM Wako Pure Chemical Corporation), supplemented with 10% fetal bovine serum (FBS; Biosera) and 1% L-glutamine solution (FUJIFILM Wako Pure Chemical Corporation). The other cell lines were cultured without antibiotics in RPMI-1640 medium, supplemented with 10% fetal bovine serum and 1% L-glutamine solution. The cells were cultured in a humidified incubator with 5% CO_2 at 37˚C. Dimethyl sulfoxide (DMSO) was used as the solvent for VP, and all the negative control groups were treated with a DMSO volume the same as the highest concentration of VP solution. Aluminum foil was used to protect cells treated with VP from light exposure, and all experiments with samples containing VP were performed in the dark.

RNA interference and transfection. YAP and TAZ were transiently knocked down in the MKN-74 and MKN-45 cell lines with validated siRNAs [L-012200-00-0005 ON-TARGETplus Human YAP1 (cat. no. 10413) siRNA-SMARTpool, L-016083-00-0005 ON-TARGETplus Human WW domain containing transcription regulator 1 (WWTR1; also known as TAZ; cat. no. 25937) siRNA-SMARTpool] from GE Healthcare Dharmacon (Horizon Discovery Group). Universal non-targeting control pool of four siRNAs (D-001810-10-05 ON-TARGETplus Non-targeting Pool) from GE Healthcare Dharmacon (Horizon Discovery Group) were used for the negative control group (NT). All the siRNA sequences used in the present study are listed in Table II. The cells were grown on 96-well or 6-well plates and transfected (final concentration, 60 nM) with Lipofectamine RNAiMAX reagent per the manufacturer's instructions (Thermo Fisher Scientific, Inc.), incubated at 37˚C for 96 h, and used for MTS assays, RT-qPCR and caspase-3/7 assays. The efficiency and specificity of the knockdown were assayed by western blotting.

Cell viability assay. VP-induced changes in gastric cancer cell viability were assessed using an MTS assay. MKN-45 and MKN-74 cells were seeded into 96-well plates at a density of $5x10^4$ cells/ml (200 μl/well) and incubated at 37˚C for 24 h. Cells were then treated with 10, 15 and 20 μM of VP and incubated at 37˚C for 24, 48 and 72 h, respectively. Cell viability was measured by MTS {3-(4,5-dimethylthiazol-2-yl)-5-[3-carboxymethoxyphenyl)-2-(4-sulfophenyl)-2H-tetrazolium] assay as follows: 100 μl of the culture medium and 20 μl of the proliferation assay solution of a CellTiter 96® AQueous One Solution Cell Proliferation assay (cat. no. G3580; Promega Corporation) were combined and incubated at 37˚C for 1 h. Absorbance was then measured at 490 nm using a microplate reader (Viento nano; Sumitomo Dainippon Pharma Co., Ltd.) with an All-in-One Microplate reader Software (Gen 5 ver 2.00.18; BioTek), and the viability of the sample relative to control cells was calculated.

Western blot analysis. MKN-45 and MKN-74 cells were treated with 15 μM of VP and incubated at 37˚C for 24 h. Whole-cell lysates were collected by adding ice-cold RIPA Lysis and Extraction Buffer (cat. no. 89900; Thermo Fisher Scientific, Inc.) containing cOmplete™ ULTRA Tablets, EASYpack Protease Inhibitor Cocktail and PhoSTOP (cat. nos. 05892970001 and 4906845001; Roche Diagnostics). Cells were collected by scraping. Samples were vortexed and lysed on ice for ~20 min. The lysed cells were centrifuged at 12,000 x g for 15 min at 4˚C to remove cellular debris. Supernatants were transferred to clean tubes, and protein concentrations were determined by a Pierce 660 nm Protein Assay Reagent (cat. no. 1861426; Thermo Fisher Scientific,

Table I. Primer sequences used for reverse transcription-quantitative PCR.

Gene	Primer sequences
Survivin	F: 5'-CAAGGACCACCGCATCTCTAC-3'
	R: 5'-AGTCTGGCTCGTTCTCAGTGG-3'
CTGF	F: 5'-CAGTGTCTGACTTCGACAACGC-3'
	R: 5'-CCATCGGCGTGTTTGGAGTA-3'
CYR61	F: 5'-GAGTGGGTCTGTGACGAGGAT-3'
	R: 5'-GGTTGTATAGGATGCGAGGCT-3'
β-actin	F: 5'-GCATCCTCACCCTGAAGTA-3'
	R: 5'-TGTGGTGCCAGATTTTCTCC-3'

CTGF, connective tissue growth factor; CYR61, Cysteine-rich angiogenic inducer 61; F, forward; R, reverse.

Table II. Sequences of siRNA oligonucleotides.

Name	Target sequences
Non-targeting	5'-UGGUUUACAUGUCGACUAA-3'
Pool (NT)	5'-UGGUUUACAUGUUGUGUGA-3'
	5'-UGGUUUACAUGUUUUCUGA-3'
	5'-UGGUUUACAUGUUUUCCUA-3'
Human YAP1	5'-GCACCUAUCACUCUCGAGA-3'
siRNA	5'-UGAGAACAAUGACGACCAA-3'
SMART pool	5'-GGUCAGAGAUACUUCUUAA-3'
(si-YAP)	5'-CCACCAAGCUAGAUAAAGA-3'
Human WWTR1	5'-CCGCAGGGCUCAUGAGUAU-3'
siRNA	5'-GGACAAACACCCAUGAACA-3'
SMART pool	5'-AGGAACAAACGUUGACUUA-3'
(si-TAZ)	5'-CCAAAUCUCGUGAUGAAUC-3'

YAP, Yes-associated protein; WWTR1, WW domain-containing transcription regulator protein 1 (alias of TAZ); TAZ, transcriptional co-activator with a PDZ-binding domain; si, small interfering.

Inc.). Proteins (30-50 μg/lane) were resolved by 4-20% SDS-PAGE and transferred to nitrocellulose membranes for western blotting. Membranes were incubated with primary antibodies at 4˚C overnight in 5% BSA-TBS Tween. Primary antibody dilutions were 1:1,000 unless otherwise indicated. Membranes were then washed for 30 min in TBS-0.05% Tween. Membranes were incubated with secondary antibodies (1:5,000) for 1 h at room temperature. Immunoreactive proteins were visualized using Clarity Western ECL substrate (cat. no. 1705061; Bio-Rad Laboratories, Inc.) and an image analyzer (LAS-3000 mini; Fujifilm Co., Ltd.) with an Image Reader (LAS-3000 UV mini ver2.2; Fujifilm Co., Ltd.). When multiple proteins were evaluated, membranes were stripped using Restore PLUS Western Blot Stripping Buffer (Thermo Fisher Scientific, Inc.) before primary antibody incubation.

Crystal violet staining. VP-induced changes in gastric cancer cell viability were also assessed by crystal violet (CV; cat. no. 031-04851; FUJIFILM Wako Pure Chemical Corporation) staining. MKN-45 and MKN-74 cells were seeded onto 6-well plates at a density of $3x10^5$ cells/ml (1 ml/well) and incubated at 37˚C for 24 h. Cells were treated with 10 and 15 μM of VP and incubated at 37˚C for 24 h. Cells were then fixed for 5 min with 4% paraformaldehyde (PFA) and stained for 30 min at room temperature with 0.05% CV. Samples were then washed twice with tap water and allowed to drain in an inverted position for ~2 min. Staining was recorded by photography, and then a volume of methanol equivalent to one-third to one-half the total well volume was added and solubilize the dye for 30 min at room temperature (20-25˚C). The absorbance at 540 nm was measured with aliquots transferred to a fresh plate using a microplate reader (Viento nano; Sumitomo Dainippon Pharma Co., Ltd.) with an All-in-One Microplate reader Software (Gen 5 ver 2.00.18; BioTek).

RNA extraction and reverse transcription-quantitative (RT-q) PCR. Total RNA was extracted from cultured cells using an miRNeasy Mini kit (cat. no. 217004; Qiagen GmbH) and quantified using a Biospec-nano spectrophotometer (Shimadzu Corporation). The extracted RNA samples were stored at -80˚C until use. cDNAs were prepared from total RNA using a High-Capacity cDNA Reverse Transcription kit (cat. no. 4374966; Thermo Fisher Scientific, Inc.) according to the manufacturer's protocols. Reverse transcription reaction mixtures contained 2 μg of total RNA, 1X RT buffer, 4 mM dNTP mix, 1X RT random primer, 50 units MultiScribe reverse transcriptase and 20 units RNase inhibitor. Nuclease-free water was added to adjust the reaction volume to 20 μl. The reaction mixtures were incubated at 25˚C for 10 min, followed by 37˚C for 120 min and 85˚C for 5 min. The real-time-PCR assays were performed in 20 μl aliquots containing 1 μl RT products with 4 μl LightCycler® FastStart DNA Master PLUS SYBR Green I (cat. no. 03515869001; Roche Diagnostics), 0.2 μl (final concentration 0.5 μM) of each primer and 14.6 μl nuclease-free water. Analyses were run on a Real-Time PCR Light Cycler® 1.5 Complete System (Roche Diagnostics). Thermal cycling was initiated with a denaturation step at 95˚C for 10 min, followed by 45 cycles of 95˚C for 10 sec, 60˚C for 10 sec, and 72˚C for 10 sec. The cycle threshold (Cq) was recorded for each target mRNA by LightCycler® Software version 3.5.28 (Roche Diagnostics), and β-actin was used as the endogenous control for data normalization. The relative expression was calculated using the formula $2^{-\Delta\Delta Cq}=2^{-(\Delta Cq, \text{reagent treatment}-\Delta Cq, \text{control})}$ (23). All the primer sequences used in the present study are listed in Table I.

Verteporfin uptake evaluation. An all-in-one fluorescence microscope (BZ-X800; Keyence Corporation) equipped with an OP-87767 filter (excitation: 405 nm and fluorescence: 630 nm) was used to evaluate VP uptake. MKN-45 and MKN-74 cells were seeded onto 96-well plates at a density of $5x10^4$ cells/ml (200 μl/well) and incubated at 37˚C for 24 h. Cells were then treated with 15 μM of VP and incubated at 37˚C for 30 min, 1 or 2 h. Pixel intensities were measured using ImageJ software ver1.52a (Wayne Rasband; National Institutes of Health) using 20 random microscopic fields (magnification, x20), according to the manufacturer's instructions (24).

Immunofluorescence. MKN-45 and MKN-74 cells were seeded on glass coverslips in 6-well plates at a density of $3x10^5$ cells/ml (1 ml/well) and incubated at 37˚C for 24 h. Cells were then treated with 15 μM of VP and incubated at 37˚C for 24 h. Cells were fixed with 4% PFA and permeabilized with 0.1% Triton X-100 and then incubated in blocking buffer containing 5.0% BSA and 0.1% glycine at room temperature (20-25˚C). Cells were incubated with the following primary antibodies in blocking buffer at 4˚C overnight; anti-YAP antibody (cat. no. sc-101199; Santa Cruz Biotechnology, Inc.), anti-TAZ antibody (cat. no. ab84927; Abcam), and anti-CD31 antibody (cat. no. ab28364; Abcam). Cells were washed and then incubated with corresponding secondary antibody, Goat anti-mouse IgG H&L (Alexa Fluor® 488; cat. no. ab150113; Abcam) in blocking buffer for 1 h at room temperature in the dark. Cells were washed, and the coverslips were mounted onto slides using ProLong Antifade Gold reagent with 4',6-diamidino-2-phenylindole (DAPI; Thermo Fisher Scientific, Inc.). Slides were analyzed with an all-in-one fluorescence microscope (BZ-X800; Keyence Corporation). Pixel intensities were measured using ImageJ software ImageJ software ver1.52a (Wayne Rasband; National Institutes of Health) using 20 random cells (magnification, x20), according to the manufacturer's instructions.

Matrigel-based tube formation assay. An aliquot of growth factor-reduced Matrigel (BD Biosciences) was warmed to room temperature, and then 50 μl/well was transferred to 24-well plates on a horizontal surface to allow even distribution. Plates were incubated for 15 min at 37˚C. MKN-45 and MKN-74 cells ($1x10^6$) were resuspended with 1 ml RPMI-1640 with 10% FBS and 20 μl of Matrigel and loaded onto the Matrigel surface in a well. VP (15 μM) was added at the same time. Each well was visualized under a microscope after 3 days at 37˚C. The average number of tubules counted manually in 10 random fields from each well was calculated.

Quantification of cell death. Cell death was evaluated by staining with an Annexin V-FITC Apoptosis Detection Kit Plus (BioVision, Inc.) and Hoechst 33342 stain (Thermo Fisher Scientific, Inc.). MKN-45 and MKN-74 cells were seeded into 96-well plates at a density of $5x10^4$ cells/ml (200 μl/well) and incubated at 37˚C for 24 h. Cells were then treated with 15 μM VP and incubated at 37˚C for 24 h. Annexin-V detection was performed according to the manufacturer's protocol. Plates were analyzed with an all-in-one fluorescence microscope (BZ-X800; Keyence Corporation). Dead cells were quantified by calculating the ratio of Annexin V and SYTOX green-positive nuclei and Hoechst 33342-positive nuclei (total nuclei) in 20 random microscopic fields (magnification, x20).

Quantification of caspase 3/7 activity. MKN-45 and MKN-74 cells were cultured on glass coverslips. When the cultures achieved the desired confluency (~50%), they were treated with siRNAs as described above. Caspase activity was evaluated by staining (incubated at 37˚C for 30 min) with a Cell Event Caspase-3/7 Green Detection Reagent (Thermo Fisher Scientific, Inc.), according to the manufacturer's protocol. Coverslips were mounted with ProLong Gold Antifade reagent with DAPI (Thermo Fisher Scientific, Inc.) and fixed overnight at room temperature in the dark. Slides were analyzed with an all-in-one fluorescence microscope (BZ-X800; Keyence Corporation). Caspase-3/7-positive cells were quantified by calculating the ratio of caspase-3/7-positive to DAPI-positive nuclei (total nuclei) in 10 random microscopic fields (magnification, x20).

Statistical analysis. All data represent ≥ three independent experiments using cells from a minimum of three separate isolations. Skewness-Kurtosis was used to check the distribution of the data. The Mann-Whitney U test was used to assess the statistical significance of differences between two groups. Kruskal-Wallis test was used for comparisons between groups and Dunn's test was applied for multiple comparisons. Survival curves were calculated using the Kaplan-Meier method on the Kaplan-Meier Plotter online tool. Statistical analyses were performed using StatFlex software (Windows ver. 6.0; Artech LLC), except for the Log-rank test for survival analysis using the Kaplan-Meier Plotter online tool. $P<0.05$ was considered to indicate a statistically significant difference and all data are expressed as the mean ± SEM.

Results

YAP and TAZ are prognostic factors of gastric cancer. YAP and TAZ expression levels in gastric cancer cells are significantly higher than those in normal tissues (Fig. 1A and B). A higher expression of YAP or TAZ in gastric cancer cells is associated with a significantly poorer prognosis than cancer cells with lower expression levels (Fig. 1C and D).

Expression patterns of YAP and TAZ differ among gastric cancer cell lines. Initially, YAP and TAZ expression levels were examined in four gastric cancer cell lines. Kato III, NUGC-4 and MKN-74 cells exhibited a YAP-dominant expression pattern. By contrast, the MKN-45 cell line showed a TAZ-dominant expression pattern (Fig. 2A). Therefore, MKN-45 was selected as the TAZ-dominant cell line and MKN-74 as the YAP-dominant cell line (Fig. S1A).

VP suppresses MKN-45 proliferation. The effect of VP on proliferation in MKN-45 and MKN-74 cells was examined using 10, 15 and 20 μM VP. VP treatment suppressed proliferation in MKN-45 cells (Fig. 2B) more than it does in MKN-74 cells at 24 h (Fig. 2C). In MKN-74 cells, the same level of proliferation suppression was observed at 72 h. VP treatment decreased the amount of CV staining in MKN-45 cells in a dose-dependent manner over 24 h (Fig. 2D). VP uptake was faster in MKN-45 cells than MKN-74 cells (Fig. 2E).

VP decreases YAP and TAZ proteins after 12 h. Western blotting demonstrated that VP treatment for 12 h reduces the expression of YAP in MKN-74 cells and TAZ in MKN-45 cells (Fig. 3A). PANC-1 cells were used as a positive control for TAZ expression (Fig. S1A).

VP decreases Surivivin gene and protein expression in MKN-45 and MKN-74 cells. VP treatment reduces the expression of downstream *Survivin* gene in MKN-45 and MKN-74 cells at 24 h (Fig. 3B and C). Moreover, immunoblotting

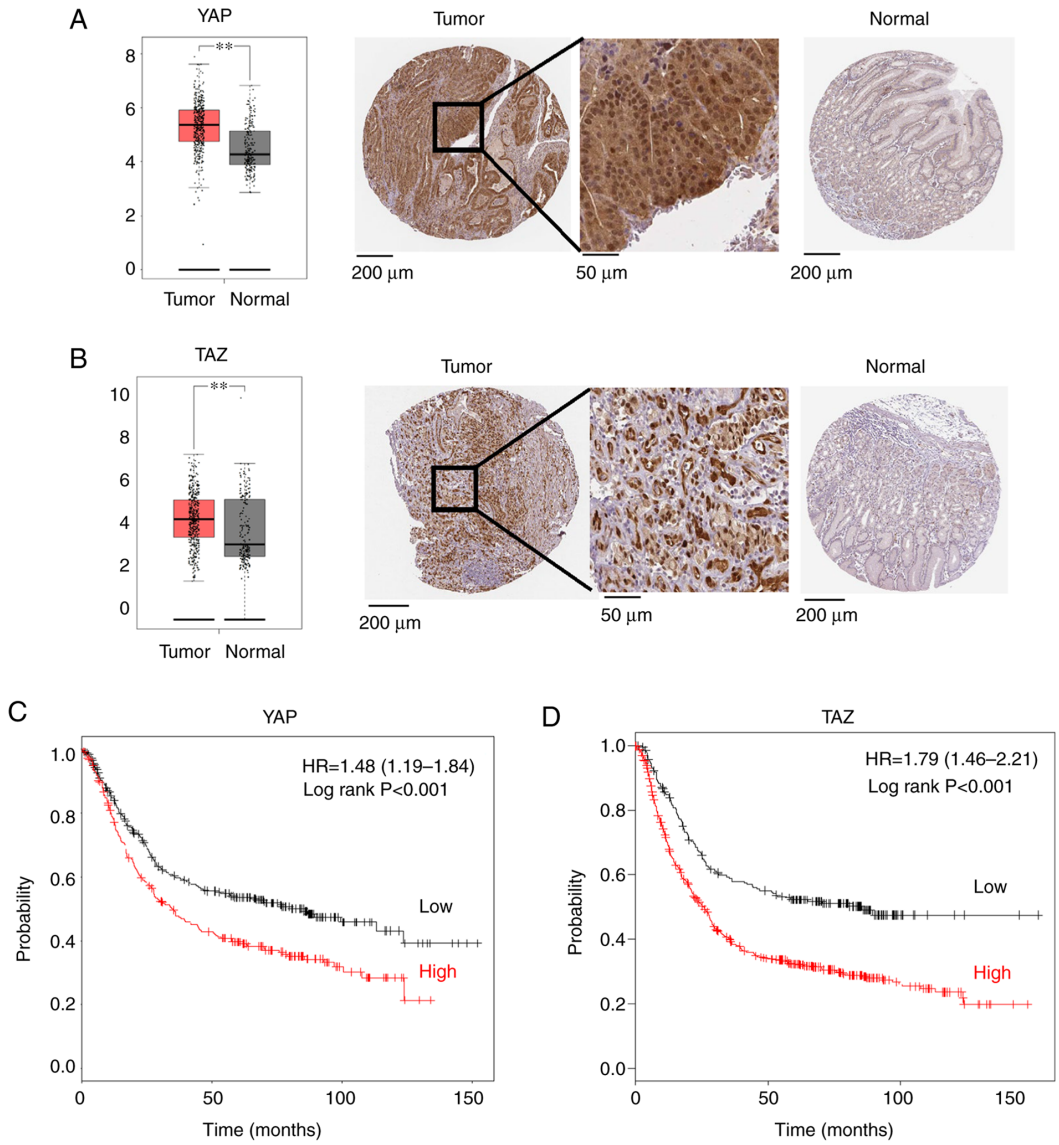

Figure 1. YAP and TAZ are prognostic factors in gastric cancer. Images from the Humap Protein Atlas showed that expression levels of (A) YAP and (B) TAZ in gastric cancer (tumor; n=408), as indicated by immunohistochemistry, were significantly higher than in the normal tissue (normal; n=211). Higher expressions of (C) YAP and (D) TAZ in gastric cancers are associated with significantly poorer prognoses relative to cancers with lower expression levels. **P<0.01 vs. control. YAP, yes-associated protein; TAZ, transcriptional co-activator with a PDZ-binding domain.

confirmed that only Survivin expression is affected by VP treatment at 24 h in both cell lines (Fig. 3D).

VP changes the localization of YAP and TAZ from nuclear to cytosolic. Immunofluorescence analysis demonstrated that exposure to 15 μM VP for 2 h changes YAP and TAZ localization from the nucleus to the cytosol in MKN-45 and MKN-74 cells (Fig. 4A and B).

VP induces cell death in MKN-45 and MKN-74 cells in a dose-dependent manner. Annexin V staining demonstrated that treatment with 15 μM of VP for 24 h induces cell death in MKN-45 and MKN-74 cells in a dose-dependent manner (Fig. 5A).

VP suppresses vascular mimicry. MKN-45 and MKN-74 are CD31-positive cells that have angiogenic and vasculogenic potential (Fig. S1B). Therefore, the vascular mimicry of both cell lines was examined using tube formation assays. In MKN-45 and MKN-74 cells, exposure to 15 μM of VP for 72 h suppressed the level vascular mimicry, demonstrated by a decrease in the number of tubules formed (Fig. 5B).

Concurrent YAP/TAZ knockdown decreases cellular proliferation. RNA interference assays targeting YAP, TAZ and YAP/TAZ in MKN-45 and MKN-74 cells demonstrated that simultaneous knockdown (YAP/TAZ) is required to decrease cell proliferation (Fig. 6A-D). YAP and YAP/TAZ knockdown also decrease *Survivin* expression. Concurrent YAP/TAZ knockdown increases caspase3/7 activity in both cell lines (Fig. 6E-G).

Discussion

In the present study, it was demonstrated that VP affects both YAP-dominant (MKN-74) and TAZ-dominant (MKN-45) cell

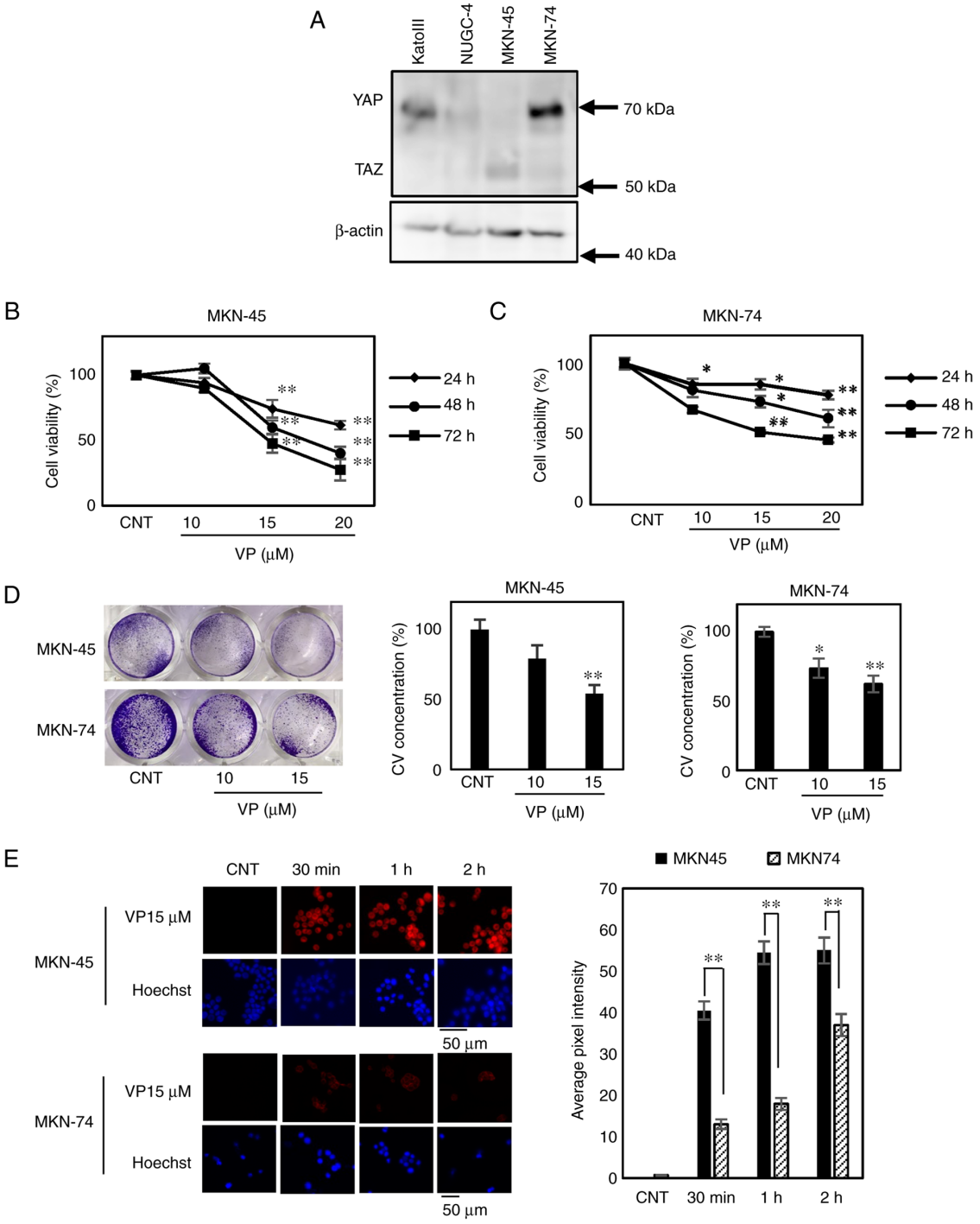

Figure 2. YAP- or TAZ-dominant gastric cancer and VP treatment. (A) Kato III, NUGC-4 and MKN-74 cells exhibited a YAP-dominant expression pattern. MKN-45 cells demonstrated a TAZ-dominant expression pattern. VP significantly suppresses the proliferation of (B) MKN-45 cells compared with (C) MKN-74 cells at 24 h, and it took 72 h to achieve the same level of proliferation suppression in MKN-74 cells. (D) VP decreased the concentration of crystal violet in MKN-45 cells in a dose-dependent manner over 24 h. (E) The uptake of VP was faster in MKN-45 cells than MKN-74 cells. The CNT group was treated with an equal volume of DMSO. *P<0.05; **P<0.01 vs. control. CNT, control; DMSO, dimethyl sulfoxide; YAP, yes-associated protein; TAZ, transcriptional co-activator with a PDZ-binding domain; VP, verteporfin.

lines. Moreover, in the poorly differentiated, TAZ-dominant gastric cancer cell line MKN-45, VP treatment elicited a more rapid suppression than in MKN-74 cells.

VP is used in PDT as a photosensitizer to eliminate abnormal blood vessels in the eyes of patients with conditions such as macular degeneration (18). It produces highly reactive, short-lived, singlet oxygen species when stimulated by non-thermal red light at 689 nm. VP has also been employed for PDT in oncology. A Phase I/II clinical trial of PDT with VP was conducted in patients with locally advanced pancreatic cancer in 2014 (25). However, light penetration into abdominal tissue is an invasive process. Therefore, the present study focused on gastric cancers because these tumors are more accessible to PDT via endoscopy. Our previous study reported the efficacy of VP in PDT using a gastric cancer cell line (19). More recently, VP has been

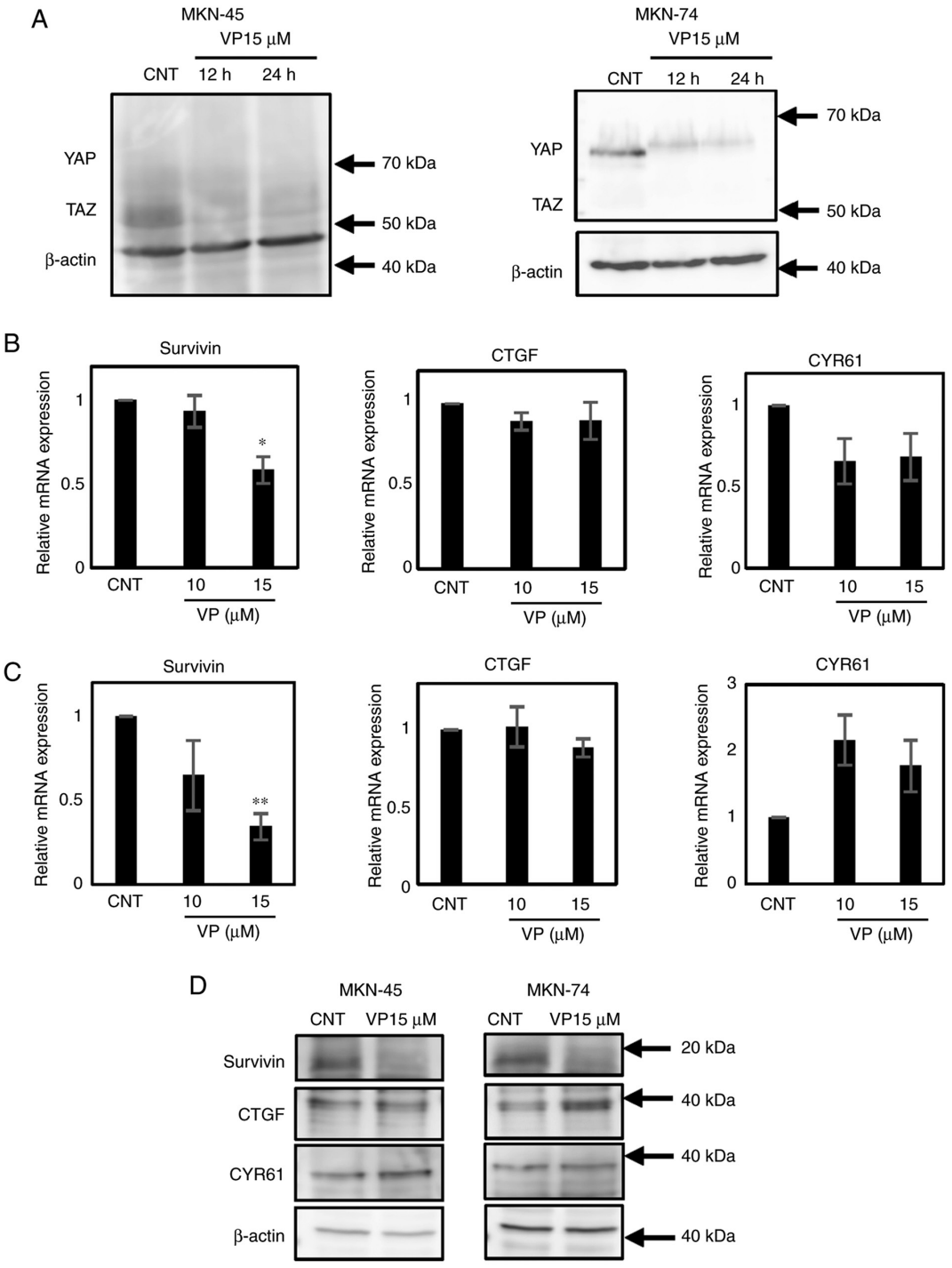

Figure 3. VP treatment significantly decreases Survivin by suppressing YAP and TAZ expression. (A) VP treatment for 12 h decreases YAP in MKN-74 cells and TAZ in MKN-45 cells, as determined by western blotting. (B) The expression of downstream genes only *Survivin* is significantly decreased in MKN-45 cells at 24 h after VP treatment. (C) In MKN-74 cells, only *Survivin* is significantly decreased at 24 h after VP treatment. (D) Immunoblotting confirms that only Survivin expression is decreased at 24 h after VP administration. The CNT group was treated with an equal volume of DMSO. *P<0.05; **P<0.01 vs. control. CNT, control; DMSO, dimethyl sulfoxide; YAP, yes-associated protein; TAZ, transcriptional co-activator with a PDZ-binding domain; VP, verteporfin; CTGF, connective tissue growth factor; CYR61, Cysteine-rich angiogenic inducer 61.

reported to have an anti-cancer effect via YAP inhibition in the absence of light activation (20-22,26,27). Moreover, VP inhibited interactions between YAP/TAZ and the TEA domain transcriptional factor (TEAD), and inhibited YAP function by upregulating the 14-3-3σ sequestering of YAP in the cytoplasm (28).

YAP and TAZ gene expression levels are elevated in a subset of human gastric cancers, most of which are associated with poor clinical outcomes (29-33). Choi *et al* (34) recently demonstrated that MYC upregulation is a direct consequence of YAP activation in YAP-activated human gastric cancer cells.

YAP and TAZ are usually discussed in the same vein. However, in renal development, YAP-knockout (KO) mice are embryonically lethal (35), whereas TAZ-knockout mice develop severe cystic kidney disease (36). A study using

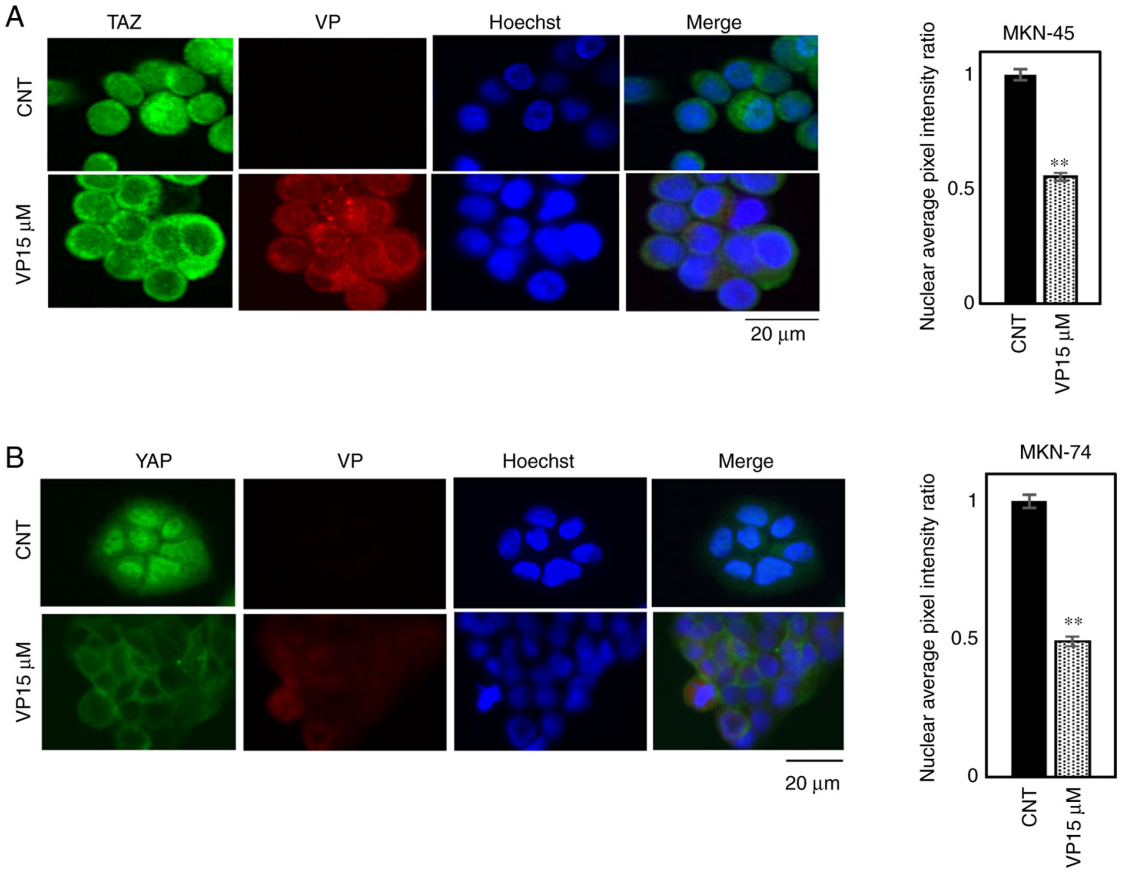

Figure 4. VP treatment changes the localization of YAP and TAZ from nuclear to cytosolic. The localization of YAP/TAZ in (A) MKN-45 and (B) MKN-74 cells changed from nuclear to cytosolic at 2 h after treatment with 15 μM VP, as shown by immunofluorescence. The CNT group was treated with an equal volume of DMSO. **P<0.01 vs. control. YAP, yes-associated protein; TAZ, transcriptional co-activator with a PDZ-binding domain; CNT, control; DMSO, dimethyl sulfoxide; VP, verteporfin.

YAP-KO, TAZ-KO and YAP-/TAZ-KO cell lines generated by the CRISPR/Cas9 technique in 293A cells revealed that YAP inactivation has more significant effects on cellular physiology than TAZ inactivation; namely, cell spreading, volume, granularity, glucose uptake, proliferation and migration (37). TAZ expression is highly elevated in gastric signet ring cell carcinoma (17). Hayashi *et al* (38) reported an imbalance in TAZ and YAP expression in gastrointestinal cancer cell lines. Another study reported that TAZ accumulation is negatively regulated by YAP abundance (39). The present results suggest that concurrent suppression of YAP and TAZ inhibits cell proliferation and that TAZ and YAP may serve distinct roles in cancer progression.

In the present study, four gastric cancer cell lines were used; one was TAZ-dominant and the other three were YAP-dominant. Kato III and NUGC-4 are signet ring carcinoma cell lines; however, YAP/TAZ dominance patterns do not depend on histological classification. VP decreases YAP and TAZ expression and subsequently reduces the expression of downstream genes, predominantly Survivin. Survivin is a new member of the inhibitor of apoptosis (IAP) family and is selectively upregulated in most human cancers but not in normal tissues (40). Moreover, it exhibits anti-apoptotic activity via caspase-3 and caspase-7 inhibition (41) and is a prognostic factor in gastric cancer associated with lymphatic metastasis (42-44). A correlation between YAP and Survivin in gastric cancer has been demonstrated for tumorigenesis and lymph node metastasis (45). The current results indicate that VP inhibits YAP/TAZ and induces apoptosis by increasing caspase-3 and caspase-7 activity via decreasing *Survivin* expression in gastric cancer cells.

Vascular mimicry (VM) is a concept proposed by Maniotis *et al* (46) in 1999. Tumors with vigorous VM are often aggressive and associated with a poor prognosis (47). Evaluating the therapeutic potential of inhibiting VM has critical clinical importance. Sun *et al* (48) demonstrated that VM is correlated with the differentiation, stage and metastatic potential of tumors, in addition to less favorable prognoses in clinical samples of gastric cancer. VP has been shown to suppress VM by disrupting the YAP-TEAD complex (49,50). CD31-positive cancer cells are reported to display VM (51), and the cell lines used in the present study were CD31-positive (Fig. S1B). Therefore, VM was evaluated in VP-treated cells using tube formation assays and it was revealed that VP significantly suppresses VM in MKN-45 and MKN-74 cells. Consequently, VP may represent a promising target for anti-cancer therapy in YAP-dominant or TAZ-dominant gastric cancers with poor prognostic outcomes.

Kang *et al* (52) demonstrated that the anti-proliferative effects of VP on gastric cancer cell lines are associated with suppression of FAT1, another marker associated with poor prognoses. Notably, more recent studies report that VP can potentially treat

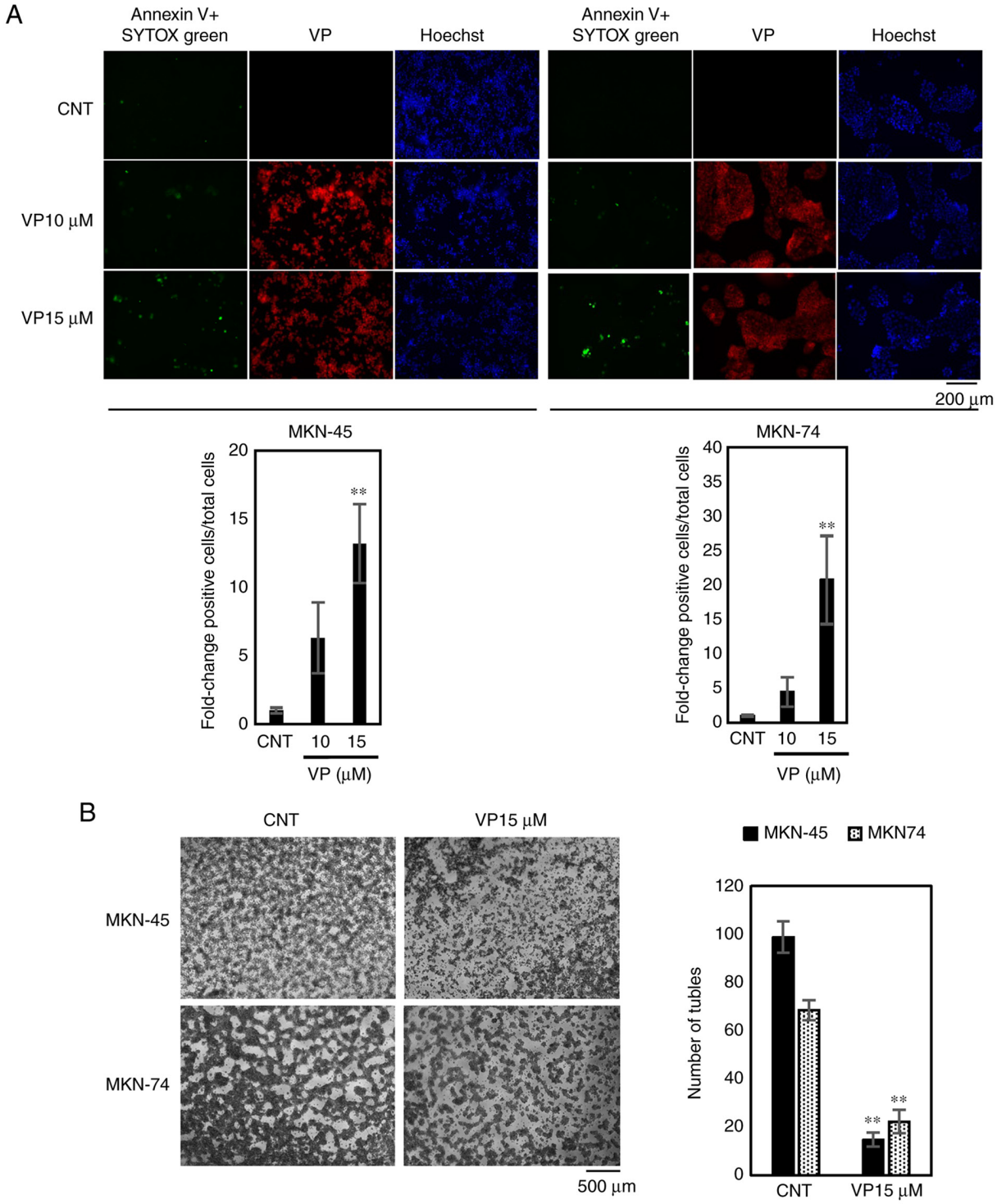

Figure 5. VP induces cell death and inhibits vascular mimicry in MKN-45 and MKN-74 cell lines. (A) Cell death is induced at 24 h after treatment with 15 μM VP, as shown by Annexin V and SYTOX green staining in MKN-45 and MKN-74 cells in a dose-dependent manner. (B) Vascular mimicry is suppressed at 72 h after treatment with 15 μM VP, as demonstrated by tube formation assays in MKN-45 and MKN-74 cells. The CNT group was treated with an equal volume of DMSO. **P<0.01 vs. control. CNT, control; DMSO, dimethyl sulfoxide; VP, verteporfin.

chemo-resistant gastric cancer stem cells (53,54). However, these studies did not distinguish between YAP and TAZ and did not evaluate the effects of VP on Survivin expression and vascular mimicry. In the present study, characteristics that reveal underlying mechanisms of VP in the suppression of gastric tumor cell growth were investigated.

One limitation of the present study was the high concentration of VP required to achieve suppression. The plasma concentration in human patients receiving liposomized VP (Visudyne®) is ~2 μg/ml. The *in vitro* assays used 10 and 15 μM VP treatments, which equate to 5 and 7.5 μg/ml, respectively, or 2-4 times more than a recommended clinical dose. Liposomization can increase VP tissue uptake, leading to a high concentration in the gastric cancer tissue.

In conclusion, VP has the potential to suppress different types of gastric cancers via suppressing Survivin. Further

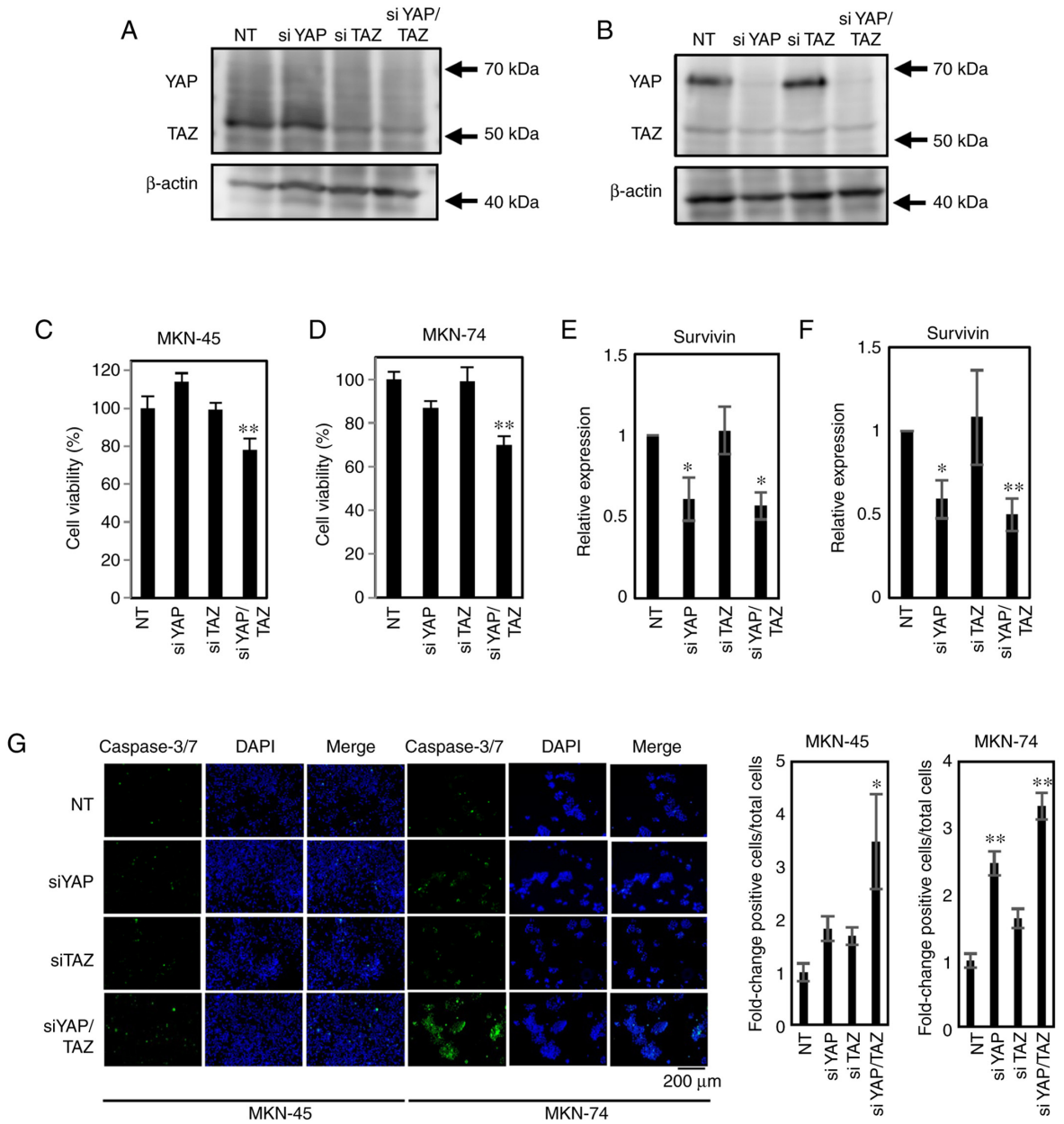

Figure 6. Concurrent YAP/TAZ knockdown decreases cell proliferation by reducing Survivin expression. RNA interference in (A) MKN-45 and (B) MKN-74 cells with siRNAs targeted against YAP (si-YAP), TAZ (si-TAZ), and YAP/TAZ (si-YAP/TAZ). Only concurrent knockdown of YAP and TAZ mRNA decreases proliferation in (C) MKN-45 and (D) MKN-74 cells, as shown by MTS assays. Knockdown of YAP and concurrent YAP/TAZ decrease the expression of *Survivin* in (E) MKN-45 and (F) MKN-74 cells. (G) Simultaneous knockdown of YAP/TAZ increases caspase 3/7 activity in MKN-45 and MKN-74 cells. *P<0.05; **P<0.01 vs. NT. NT, non-targeting siRNA; YAP, yes-associated protein; TAZ, transcriptional co-activator with a PDZ-binding domain; VP, verteporfin; si, small interfering.

in vivo studies will be required to confirm the potential of VP for use as a therapeutic agent.

Acknowledgements

Not applicable.

Funding

The resources and facilities of the Faculty of Medicine, Tottori University were used to conduct this study. This research did not receive any specific grant from funding agencies in the public, commercial or not-for-profit sectors.

Availability of data and materials

The datasets used and analyzed in this study are available from the corresponding author upon reasonable request.

Authors' contributions

TH, TS, YH, RT, YM, and TK designed and implemented the experiments. TS, TT, TN, and TM searched the literature and analyzed and interpreted the data. TS, TT, TN, and TM were also involved in writing, reviewing, and editing the manuscript. HI made substantial contributions to the conception and design of the project and gave final approval of the

version to be published. TH and TS confirmed the authenticity of all the raw data. All authors read and approved the final manuscript.

Ethics approval and consent to participate

Not applicable.

Patient consent for publication

Not applicable.

Competing interests

The authors declare that they have no competing interests.

References

1. Sung H, Ferlay J, Siegel RL, Laversanne M, Soerjomataram I, Jemal A and Bray F: Global cancer statistics 2020: GLOBOCAN Estimates of incidence and mortality worldwide for 36 cancers in 185 countries. CA Cancer J Clin 71: 209-249, 2021.
2. Sitarz R, Skierucha M, Mielko J, Offerhaus GJA, Maciejewski R and Polkowski WP: Gastric cancer: Epidemiology, prevention, classification and treatment. Cancer Manag Res 10: 239-248, 2018.
3. Takahashi T, Saikawa Y and Kitagawa Y: Gastric cancer: Current status of diagnosis and treatment. Cancers (Basel) 5: 48-63, 2013.
4. Sugano K: Screening of gastric cancer in Asia. Best Pract Res Clin Gastroenterol 29: 895-905, 2015.
5. Japanese Gastric Cancer Association: Japanese gastric cancer treatment guidelines 2014 (ver. 4). Gastric Cancer 20: 1-19, 2017.
6. Wagner AD, Syn NL, Moehler M, Grothe W, Yong WP, Tai BC, Ho J and Unverzagt S: Chemotherapy for advanced gastric cancer. Cochrane Database Syst Rev 8: CD004064, 2017.
7. Pan D: Hippo signaling in organ size control. Genes Dev 21: 886-897, 2007.
8. Zanconato F, Cordenonsi M and Piccolo S: YAP/TAZ at the roots of cancer. Cancer Cell 29: 783-803, 2016
9. Zhang J, Xu ZP, Yang YC, Zhu JS, Zhou Z and Chen WX: Expression of yes-associated protein in gastric adenocarcinoma and inhibitory effects of its knockdown on gastric cancer cell proliferation and metastasis. Int J Immunopathol Pharmacol 25: 583-590, 2012.
10. Zanconato F and Piccolo S: Eradicating tumor drug resistance at its YAP -biomechanical roots. EMBO J 35: 459-461, 2016.
11. Zhou Y, Wang Y, Zhou W, Chen T, Wu Q, Chutturghoon VK, Lin B, Geng L, Yang Z, Zhou L and Zheng S: YAP promotes multi-drug resistance and inhibits autophagy-related cell death in hepatocellular carcinoma via the RAC1-ROS-mTOR pathway. Cancer Cell Int 19: 179, 2019.
12. Song J, Xie LX, Zhang XY, Hu P, Long MF, Xiong F, Huang J and Ye XQ: Role of YAP in lung cancer resistance to cisplatin. Oncol Lett 16: 3949-3954, 2018.
13. Song R, Gu D, Zhang L, Zhang X, Yu B, Liu B and Xie J: Functional significance of Hippo/YAP signaling for drug resistance in colorectal cancer. Mol Carcinog 57: 1608-1615, 2018.
14. Lu T, Sun L and Zhu X: Yes-associated protein enhances proliferation and attenuates sensitivity to cisplatin in human gastric cancer cells. Biomed Pharmacother 105: 1269-1275, 2018.
15. Shi J, Li F, Yao X, Mou T, Xu Z, Han Z, Chen S, Li W, Yu J, Qi X, *et al*: The HER4-YAP1 axis promotes trastuzumab resistance in HER2-positive gastric cancer by inducing epithelial and mesenchymal transition. Oncogene 37: 3022-3038, 2018.
16. Hu X, Xin Y, Xiao Y and Zhao J: Overexpression of YAP1 is correlated with progression, metastasis and poor prognosis in patients with gastric carcinoma. Pathol Oncol Res 20: 805-811, 2014.
17. Yue G, Sun X, Gimenez-Capitan A, Shen J, Yu L, Teixido C, Guan W, Rosell R, Liu B and Wei J: TAZ is highly expressed in gastric signet ring cell carcinoma. Biomed Res Int 2014: 393064, 2014.
18. Cruess AF, Zlateva G, Pleil AM and Wirostko B: Photodynamic therapy with verteporfin in age-related macular degeneration: A systematic review of efficacy, safety, treatment modifications and pharmacoeconomic properties. Acta Ophthalmol 87: 118-132, 2009.
19. Mae Y, Kanda T, Sugihara T, Takata T, Kinoshita H, Sakaguchi T, Hasegawa T, Tarumoto R, Edano M, Kurumi H, *et al*: Verteporfin-photodynamic therapy is effective on gastric cancer cells. Mol Clin Oncol 13: 10, 2020.
20. Dasari VR, Mazack V, Feng W, Nash J, Carey DJ and Gogoi R: Verteporfin exhibits YAP-independent anti-proliferative and cytotoxic effects in endometrial cancer cells. Oncotarget 8: 28628-28640, 2017.
21. Al-Moujahed A, Brodowska K, Stryjewski TP, Efstathiou NE, Vasilikos I, Cichy J, Miller JW, Gragoudas E and Vavvas DG: Verteporfin inhibits growth of human glioma in vitro without light activation. Sci Rep 7: 7602, 2017.
22. Dong L, Lin F, Wu W, Liu Y and Huang W: Verteporfin inhibits YAP-induced bladder cancer cell growth and invasion via Hippo signaling pathway. Int J Med Sci 15: 645-652, 2018.
23. Livak KJ and Schmittgen TD: Analysis of relative gene expression data using real-time quantitative PCR and the 2(-Delta Delta C(T)) method. Methods 25: 402-408, 2001.
24. Schneider CA, Rasband WS and Eliceiri KW: NIH image to imageJ: 25 years of image analysis. Nat Methods 9: 671-675, 2012.
25. Huggett MT, Jermyn M, Gillams A, Illing R, Mosse S, Novelli M, Kent E, Bown SG, Hasan T, Pogue BW and Pereira SP: Phase I/II study of verteporfin photodynamic therapy in locally advanced pancreatic cancer. Br J Cancer 110: 1698-1704, 2014.
26. Brodowska K, Al-Moujahed A, Marmalidou A, Meyer Zu Horste M, Cichy J, Miller JW, Gragoudas E and Vavvas DG: The clinically used photosensitizer Verteporfin (VP) inhibits YAP-TEAD and human retinoblastoma cell growth in vitro without light activation. Exp Eye Res 124: 67-73, 2014.
27. Feng J, Gou J, Jia J, Yi T, Cui T and Li Z: Verteporfin, a suppressor of YAP-TEAD complex, presents promising antitumor properties on ovarian cancer. Onco Targets Ther 9: 5371-5381, 2016.
28. Wang C, Zhu X, Feng W, Yu Y, Jeong K, Guo W, Lu Y and Mills GB: Verteporfin inhibits YAP function through up-regulating 14-3-3σ sequestering YAP in the cytoplasm. Am J Cancer Res 6: 27-37, 2015.
29. Kang W, Tong JH, Chan AW, Lee TL, Lung RW, Leung PP, So KK, Wu K, Fan D, Yu J, *et al*: Yes-associated protein 1 exhibits oncogenic property in gastric cancer and its nuclear accumulation associates with poor prognosis. Clin Cancer Res 17: 2130-2139, 2011.
30. Li P, Sun D, Li X, He Y, Li W, Zhao J, Wang Y, Wang H and Xin Y: Elevated expression of Nodal and YAP1 is associated with poor prognosis of gastric adenocarcinoma. J Cancer Res Clin Oncol 142: 1765-1773, 2016.
31. Hong SA, Son MW, Cho J, Jang SH, Lee HJ, Lee JH, Cho HD, Oh MH and Lee MS: Low angiomotin-p130 with concomitant high Yes-associated protein 1 expression is associated with adverse prognosis of advanced gastric cancer. APMIS 125: 996-1006, 2017.
32. Huang S, Zhu L, Cao Y, Li L, Xie Y, Deng J and Xiong J: Significant association of YAP1 and HSPC111 proteins with poor prognosis in Chinese gastric cancer patients. Oncotarget 8: 80303-80314, 2017.
33. Zhang L, Song X, Li X, Wu C and Jiang J: Yes-Associated protein 1 as a novel prognostic biomarker for gastrointestinal cancer: A meta-analysis. Biomed Res Int 2018: 4039173, 2018.
34. Choi W, Kim J, Park J, Lee DH, Hwang D, Kim JH, Ashktorab H, Smoot D, Kim SY, Choi C, *et al*: YAP/TAZ initiates gastric tumorigenesis via upregulation of MYC. Cancer Res 78: 3306-3320, 2018.
35. Morin-Kensicki EM, Boone BN, Howell M, Stonebraker JR, Teed J, Alb JG, Magnuson TR, O'Neal W and Milgram SL: Defects in yolk sac vasculogenesis, chorioallantoic fusion, and embryonic axis elongation in mice with targeted disruption of Yap65. Mol Cell Biol 26: 77-87, 2006.
36. Tian Y, Kolb R, Hong JH, Carroll J, Li D, You J, Bronson R, Yaffe MB, Zhou J and Benjamin T: TAZ promotes PC2 degradation through a SCFbeta-Trcp E3 ligase complex. Mol Cell Biol 27: 6383-6395, 2007.
37. Plouffe SW, Lin KC, Moore JL III, Tan FE, Ma S, Ye Z, Qiu Y, Ren B and Guan KL: The Hippo pathway effector proteins YAP and TAZ have both distinct and overlapping functions in the cell. J Biol Chem 293: 11230-11240, 2018.
38. Hayashi H, Higashi T, Yokoyama N, Kaida T, Sakamoto K, Fukushima Y, Ishimoto T, Kuroki H, Nitta H, Hashimoto D, *et al*: An imbalance in TAZ and YAP expression in hepatocellular carcinoma confers cancer stem cell-like behaviors contributing to disease progression. Cancer Res 75: 4985-4997, 2015.

39. Finch-Edmondson ML, Strauss RP, Passman AM, Sudol M, Yeoh GC and Callus BA: TAZ protein accumulation is negatively regulated by YAP abundance in mammalian cells. J Biol Chem 290: 27928-27938, 2015.
40. Altieri DC: Survivin, versatile modulation of cell division and apoptosis in cancer. Oncogene 22: 8581-8589, 2003.
41. Tamm I, Wang Y, Sausville E, Scudiero DA, Vigna N, Oltersdorf T and Reed JC: IAP-family protein survivin inhibits caspase activity and apoptosis induced by Fas (CD95), Bax, caspases, and anti-cancer drugs. Cancer Res 58: 5315-5320, 1998.
42. Cerda-Opazo P, Valenzuela-Valderrama M, Wichmann I, Rodríguez A, Contreras-Reyes D, Fernández EA, Carrasco-Aviño G, Corvalán AH and Quest AFG: Inverse expression of survivin and reprimo correlates with poor patient prognosis in gastric cancer. Oncotarget 9: 12853-12867, 2018.
43. Bertazza L, Mocellin S, Marchet A, Pilati P, Gabrieli J, Scalerta R and Nitti D: Survivin gene levels in the peripheral blood of patients with gastric cancer independently predict survival. J Transl Med 7: 111, 2009.
44. Zhang J, Zhu Z, Sun Z, Sun X, Wang Z and Xu H: Survivin gene expression increases gastric cancer cell lymphatic metastasis by up-regulating vascular endothelial growth factor-C expression levels. Mol Med Rep 9: 600-606, 2014.
45. Da C, Xin Y, Zhao J and Luo X: Significance and relationship between Yes-associated protein and survivin expression in gastric carcinoma and precancerous lesions. World J Gastroenterol 15: 4055-4061, 2009.
46. Maniotis AJ, Folberg R, Hess A, Seftor EA, Gardner LM, Pe'er J, Trent JM, Meltzer PS and Hendrix MJ: Vascular channel formation by human melanoma cells in vivo and in vitro: Vasculogenic mimicry. Am J Pathol 155: 739-752, 1999.
47. Zhang S, Zhang D and Sun B: Vasculogenic mimicry: Current status and future prospects. Cancer Lett 254: 157-164, 2007.
48. Sun J, Sun B, Sun R, Zhu D, Zhao X, Zhang Y, Dong X, Che N, Li J, Liu F, *et al*: HMGA2 promotes vasculogenic mimicry and tumor aggressiveness by up-regulating Twist1 in gastric carcinoma. Sci Rep 7: 2229, 2017.
49. Bora-Singhal N, Nguyen J, Schaal C, Perumal D, Singh S, Coppola D and Chellappan S: YAP1 regulates OCT4 activity and SOX2 expression to facilitate self-renewal and vascular mimicry of stem-like cells. Stem Cells 33: 1705-1718, 2015.
50. Wei H, Wang F, Wang Y, Li T, Xiu P, Zhong J, Sun X and Li J: Verteporfin suppresses cell survival, angiogenesis and vasculogenic mimicry of pancreatic ductal adenocarcinoma via disrupting the YAP-TEAD complex. Cancer Sci 108: 478-487, 2017.
51. Kim HS, Won YJ, Shim JH, Kim HJ, Kim J, Hong HN and Kim BS: Morphological characteristics of vasculogenic mimicry and its correlation with EphA2 expression in gastric adenocarcinoma. Sci Rep 9: 3414, 2019.
52. Kang MH, Jeong GS, Smoot DT, Ashktorab H, Hwang CM, Kim BS, Kim HS and Park YY: Verteporfin inhibits gastric cancer cell growth by suppressing adhesion molecule FAT1. Oncotarget 8: 98887-98897, 2017.
53. Xiong J, Wang S, Chen T, Shu X, Mo X, Chang G, Chen JJ, Li C, Luo H and Lee JD: Verteporfin blocks Clusterin which is required for survival of gastric cancer stem cell by modulating HSP90 function. Int J Biol Sci 15: 312-324, 2019.
54. Giraud J, Molina-Castro S, Seeneevassen L, Sifré E, Izotte J, Tiffon C, Staedel C, Boeuf H, Fernandez S, Barthelemy P, *et al*: Verteporfin targeting YAP1/TAZ-TEAD transcriptional activity inhibits the tumorigenic properties of gastric cancer stem cells. Int J Cancer 146: 2255-2267, 2020.